

# Effect of clay contents on mechanical and water vapor barrier properties of agar-based nanocomposite films

Jong-Whan Rhim\*

Department of Food Engineering, Mokpo National University, 960 Muanro, Chungkyemyon, Muangun, 534-729 Jeonnam, Republic of Korea

## ARTICLE INFO

### Article history:

Received 31 January 2011

Received in revised form 4 May 2011

Accepted 11 May 2011

Available online 18 May 2011

### Keywords:

Agar

Nanocomposite films

Clay content

Mechanical properties

Water vapor barrier properties

## ABSTRACT

Agar/clay (Cloisite Na<sup>+</sup>) nanocomposite films with different amount of the nanoclay (0, 2.5, 5, 10, 15, and 20 g clay/100 g agar) were prepared using a solution intercalation method. Results on X-ray diffraction (XRD) and scanning electron microscopy (SEM) revealed well developed intercalated nanocomposite films especially at low level of nanoclay addition, and their properties were greatly influenced with the clay content. Tensile strength (TS) increased with increase in the clay content up to 10%, and decreased with more than 10% of clay incorporation. Water vapor permeability (WVP), water vapor uptake ratio (WVUR<sub>5</sub>), and water solubility (WS) decreased with increase in the nanoclay content due to the tortuous path for water vapor diffusion and strong structure formed between the intercalated silicate layers and the polymer matrix. Hydrophilicity of the nanocomposite films increased with increase in the hydrophilic nanoclay, resulted in decreased water contact angle (CA) and increased swelling ratio (SR).

© 2011 Elsevier Ltd. All rights reserved.

## 1. Introduction

Concerns on environmental impact and exhausting natural resources caused by non-biodegradable petrochemical-based plastic packaging materials have led to a renewed interest on biopolymer-based packaging materials (Siracusa, Rocculi, Romani, & Rossa, 2008; Weber, Haugaard, Festersen, & Bertelsen, 2002). The use of biopolymer-based packaging materials is expected to solve these problems to a certain extent. Such biopolymers are usually derived from annually renewable natural resources including carbohydrates and proteins of plant or animal origin (Boredes, Pollet, & Avérous, 2009). As one of such renewable source-based biodegradable packaging materials, agar has been tested as an alternative source for the non-biodegradable and nonrenewable plastic packaging materials since it is thermoplastic, biodegradable, biocompatible and has high mechanical strength with moderate water resistance (Freile-Pelegrín et al., 2007; Phan, Debeaufort, Luu, & Voilley, 2005; Phan, Debeaufort, Voilley, & Luu, 2009; Wu, Geng, Chang, Yu, & Ma, 2009). Agar is a fibrous carbohydrate extracted from a number of marine algae of the class *Rhodophyceae*, called 'red seaweeds', such as *Gelidium sp.* and *Gracilaria sp.* It is composed of  $\beta$ -D-galactopyranosyl linked (1  $\rightarrow$  4) to a 3,6-anhydro- $\alpha$ -L-galactopyranosyl unit with partially sulfated, and it produces perceptible gels at concentrations as low as 0.04% (Labropoulos, Niesz, Danforth, & Kevrekidis, 2002). Agar has been tested to pre-

pare environmentally friendly packaging materials such as foams, films and coatings (Freile-Pelegrín et al., 2007; Lee, Lee, & Song, 1997; Phan et al., 2005, 2009), and added to other biopolymers such as milk protein (Letendre, D'Aprano, Lacroix, & Salmieri, 2002) and starch (Wu et al., 2009) to improve mechanical and water vapor barrier properties. However, brittleness and other properties such as low thermal stability, medium gas barrier properties and low water resistance of the pure biopolymer are often insufficient for food packaging applications (Cabedo, Feijoo, Villanueva, Lagarón, & Giménez, 2006; Sorrentino, Gorrasi, & Vittoria, 2007).

Recently, a new class of materials represented by bionanocomposites has been suggested as a promising option in improving mechanical and barrier properties of biopolymer-based packaging materials (Pandey et al., 2005; Pavlidou and Papaspyrides, 2008; Rhim and Ng, 2007; Sinha Ray and Bousmina, 2005). Nanocomposite is a hybrid material consisting of polymer matrix reinforced with nano-scale fillers having at least one dimension in the nanometer range. Generally, 2:1 layered silicate (or 2:1 phyllosilicates) clays such as montmorillonite, saponite or hectorite are used as nanofiller for the preparation of nanocomposite in the packaging sector since they are environmentally friendly, non-toxic and abundant in nature (Alexandre and Dubois, 2000). A well developed nanocomposite, in which nanoclays are evenly dispersed in the state of intercalated or exfoliated in the polymer matrix, exhibits significant improvements to the polymer matrix in terms of mechanical, gas barrier, solvent resistance, and optical properties at low filler content (less than 5% by weight) (Alexandre and Dubois, 2000; Brody, 2003; Pandey et al., 2005; Pavlidou and Papaspyrides, 2008; Rhim and Ng, 2007; Sinha Ray and Bousmina,

\* Corresponding author. Tel.: +82 61 450 2423; fax: +82 61 454 1521.

E-mail address: [jwrhim@mokpo.ac.kr](mailto:jwrhim@mokpo.ac.kr)

2005). Formation of nanocomposites and the resulting property enhancements are known to depend not only on the compatibility between nanofillers and polymer matrix, but also on the clay types and their concentration and on their preparation methods (Arora and Padua, 2009; Pavlidou and Papaspyrides, 2008; Rhim et al., 2006).

Various natural biopolymers, including carbohydrates such as cellulose (Park et al., 2004; Petersson and Oksman, 2006), starch (Avella et al., 2005; Cyras et al., 2008; Park et al., 2002), and chitosan (De Mesquita et al., 2010; Rhim et al., 2006), and proteins such as soy protein (Kumar et al., 2010a,b), gelatin (Bae et al., 2009; Rao, 2007), wheat gluten (Mauricio-Iglesias et al., 2010; Tunc et al., 2007), and whey protein (Hedenqvist et al., 2006; Sothornvit et al., 2010; Zhou et al., 2009) have been tested to exploit the property enhancement through the formation of nanocomposites. However, only a few studies on the preparation of agar-based nanocomposite films have been performed (Jang et al., 2010; Rhim, Lee, & Hong, 2011). Jang et al. (2010) prepared nanocomposite films using freeze-dried powder of hot water extracted red algae (*Gelidium corneum*) and nanoclay (Cloisite Na<sup>+</sup>) to improve the physical properties of the film. Rhim et al. (2011) prepared agar-based nanocomposite films using food grade agar and three different types of nanoclays, i.e., a natural montmorillonite (Cloisite Na<sup>+</sup>) and two organoclays (Cloisite 30B and Cloisite 20A), and reported that the clay types played a crucial role to the formation of nanocomposite and properties of the polymer/clay nanocomposite. They found that the hydrophilic Cloisite Na<sup>+</sup> was the most compatible with agar polymer matrix as evidenced by the XRD results and the physical properties such as transparency, mechanical, water vapor barrier, and other water resistance properties.

By the way, the performance properties of the biopolymer/clay nanocomposites are dependent on various factors such as compatibility between polymer matrix and type of nanoclays (Rhim et al., 2011), nanocomposite preparation methods (Müller et al., 2011) and nanoclay content (Sothornvit et al., 2010). Therefore, it is very important to test the effect of clay content to determine the optimum concentration of nanoclay in order to prepare nanocomposite films with desired film properties for the packaging application.

The main objective of this study was therefore to investigate the effect of content of nanoclays on the packaging film properties such as the mechanical, water vapor barrier, water resistance properties of the prepared agar-based nanocomposite films.

## 2. Materials and methods

### 2.1. Materials

Food grade agar was obtained from Fine Agar Agar Co., Ltd. (Damyang, Jeonnam, Korea). An unmodified natural montmorillonite (Cloisite Na<sup>+</sup>: cation exchange capacity of 92 meq/100 g) was purchased from Southern Clay (Gonzales, TX, USA). Glycerin was purchased from Daejung Chemicals & Metals Co., Ltd. (Siheung, Gyonggido, Korea).

### 2.2. Preparation of films

Agar and agar-based nanocomposite films were prepared using a solvent casting method proposed by Rhim et al. (2011). Film solutions were prepared by dissolving 4 g of agar in 150 mL of distilled water with 2 g of glycerin as plasticizer while mixing vigorously for 30 min at 95 °C using a magnetic stirrer. The film solution was cast evenly onto a leveled Teflon film (Cole-Parmer Instrument Co., Chicago, IL, USA) coated glass plate (24 cm × 30 cm), then dried for about 24 h at room temperature and the resultant film was peeled from the casting surface. In addition, agar nanocomposite films

with various clay contents, 2.5, 5, 10, 15, and 20% (part clay per 100 part agar), were prepared using a solution intercalation method (Rhim et al., 2011). First, precisely weighed nanoclay (Cloisite Na<sup>+</sup>) was dispersed into distilled water (150 mL) and stirred using a magnetic stirrer for 24 h to reach complete swelling of the clay. The fully hydrated nanoclay solution was homogenized using a high shear mixer (T25 basic, Ika Labortechnik, Janke & Kunkel GmbH & Co., KG Staufen, Germany) at 20,500 rpm for 10 min followed by sonication for 10 min using a High Intensity Ultrasonic Processor (Model VCX 750, Sonics & Materials Inc., Newtown, CT, USA) with medium size tip (2 cm diameter). Four grams of agar and 2 g of glycerin were then dissolved into the nanoclay solutions and heated for 30 min at 95 °C with vigorous mixing using a magnetic stirrer, cast onto the glass plate and followed by the same procedures, as described above.

### 2.3. Film thickness and conditioning

Test films were cut into 7 cm × 7 cm and 2.54 cm × 15 cm-sized pieces for the measurement of water vapor permeability (WVP) and transmittance, and tensile properties, respectively. Film thickness was measured using a micrometer (Dial Thickness gauge 7301, Mitutoyo, Japan) at an accuracy of 0.01 mm. All the film samples were preconditioned in a constant temperature humidity chamber set at 25 °C and 50% RH for at least 48 h.

### 2.4. Transparency

Film transparency was determined by measuring the percent transmittance at 660 nm using a UV/VIS spectrophotometer (Model 8451A, Hewlett–Packard Co., Santa Alara, CA, USA) (Rhim et al., 2006).

### 2.5. Surface morphology

Surface morphology of the agar and agar/Cloisite Na<sup>+</sup> nanocomposite films were observed using a FE-SEM (Field Effect Scanning Electron Microscope; S-4800, Hitachi Co., Ltd., Matsuda, Japan) operated at  $V_{acc} = 1$  kV and  $I_e = 10$   $\mu$ A.

### 2.6. XRD pattern

XRD patterns of the nanoclay and agar/clay nanocomposite films were taken with a PANalytical Xpert pro MRD diffractometer (Amsterdam, Netherlands), operated at 40 kV and 30 mA, equipped with Cu K $\alpha$  radiation at a wavelength of 0.1546 nm and a curved graphite crystal monochromator. Samples were scanned over the range of diffraction angle of  $2\theta = 1 - 10^\circ$  with a scanning rate of  $0.4^\circ/\text{min}$  at room temperature. The basal spacing of the silicate layer ( $d_{001}$ ) was calculated using the Bragg's diffraction equation,  $\lambda = 2d \sin \theta$ , where  $\lambda$  is the wavelength of the X-ray radiation used (0.1546 nm),  $d$  is the spacing between diffraction lattice planes and  $\theta$  is the measured diffraction angle.

### 2.7. Surface roughness

Three dimensional images of the films were observed using an AFM (Atomic Force Microscope; also called SPM: Scanning Probe Microscope; XE-100, Park AFM Co, Ltd., Suwon, Korea) in non-contact mode with scan size of 20  $\mu$ m.

### 2.8. Tensile properties

Tensile properties such as tensile strength (TS) and elongation at break (E) of each film were evaluated with a Model 5565

Instron Universal Testing Machine (Instron Engineering Corporation, Canton, MA, USA) using an ASTM Method D 882-88. Initial grip separation was set at 50 mm and cross-head speed at 50 mm/min.

### 2.9. Water vapor permeability (WVP)

WVP ( $\text{g m}^{-2} \text{s Pa}$ ) of agar and agar/clay nanocomposite films was calculated as:

$$\text{WVP} = \frac{\text{WVTR} \times L}{\Delta p} \quad (1)$$

where WVTR was the measured water vapor transmission rate ( $\text{g m}^{-2} \text{s}$ ) through a film,  $L$  was the mean film thickness (m) and  $\Delta p$  was the partial water vapor pressure difference (Pa) across the two sides of the film. WVTR was determined gravimetrically using a modified ASTM Method E 96-95. Film specimens were mounted horizontally on poly(methylmethacrylate) cups filled with distilled water up to 1 cm underneath the film. The cups were placed in an environmental chamber at 25 °C and 50% RH with air current movement at 198 m/min. The cups were weighed every hour for a period of 8 h. The slopes of the steady state (linear) portion of weight loss versus time curves were used to calculate WVTR. In calculating WVP, effect of the resistance of the stagnant air layer between the film undersides and the surface of the water in the cups was corrected using the method of Gennadios et al. (1994).

### 2.10. Water contact angle (CA)

The CA of water in air on the film surface was measured with a CA analyzer (model Phenix 150, Surface Electro Optics Co., Ltd., Kunpo, Korea) after a water drop of ca. 10  $\mu\text{L}$  was placed on the surface of film using a microsyringe. All film samples (3 cm  $\times$  10 cm) were glued on the movable sample plate (black Teflon coated steel, 7 cm  $\times$  11 cm) leveled horizontally before measurement. The CA on both sides of the drop was measured to assume symmetry and horizontal level.

### 2.11. Water resistance

Water solubility (WS) of films was determined as the percentage of soluble matter to the initial dry matter of film sample (Gontard et al., 1992). Three randomly selected specimens from each type of film were first dried at 105 °C for 24 h to determine initial dry matter. Separate films were immersed in 30 mL of distilled water in a 50 mL beaker. Beakers were covered with Parafilm "M" wrap (American National Can, Greenwich, CT) and stored in an environmental chamber at 25 °C for 24 h with occasional stirring. Undissolved dry matter was determined by removing the film pieces from the beakers, gently rinsing them with distilled water, and then oven drying them (105 °C, 24 h). The weight of solubilized matter was calculated by subtracting the weight of unsolubilized matter from the weight of initial dry matter and expressed as a percentage of the initial dry matter content.

Swelling ratio (SR) of films was determined gravimetrically. Pre-weighed squared specimens (25.4 mm  $\times$  50 mm) were immersed in distilled water. Samples were then removed at specified intervals and weighed after removing the surface water with blotting paper. The SR was calculated as follows:

$$\text{SR}(\%) = \frac{m_t - m_o}{m_o} \times 100 \quad (2)$$

where  $m_o$  and  $m_t$  are the weight of the samples before and after immersion, respectively. The SR of the film samples were determined after immersion them in distilled water for 30 min and 24 h.

Water vapor uptake ratio (WVUR) was determined following the method of Tunc et al. (2007). Squared samples (25.4 mm  $\times$  50 mm) were first dried in a vacuum drier at 60 °C for 1 day. After being

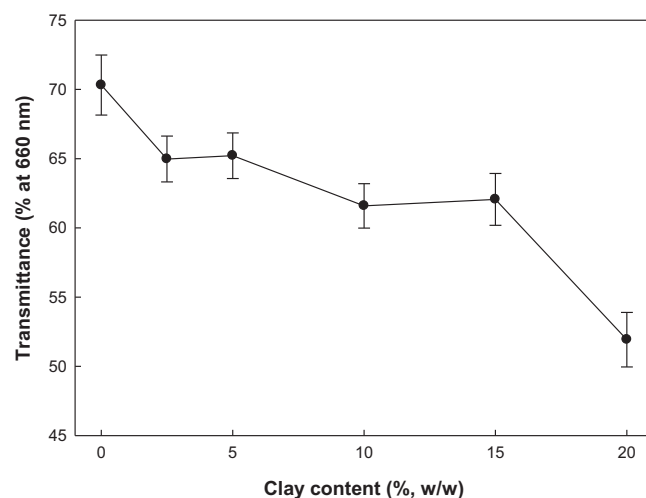


Fig. 1. Effect of clay content on transmittance of agar/Cloisite Na<sup>+</sup> nanocomposite films.

weighed using a four-digit electronic balance, the samples were stored over K<sub>2</sub>SO<sub>4</sub> saturated salt (98% RH) for 5 days (WVUR<sub>5</sub>). The WVUR was calculated as:

$$\text{WVUR}(\%) = \frac{m_t - m_o}{m_o} \times 100 \quad (3)$$

where  $m_o$  and  $m_t$  are the weight of the samples before and after water vapor absorption, respectively.

### 2.12. Data analysis

The measurements of all the film properties (TS, E, transmittance, WVP, WS, SR, and WVUR) were measured with individually prepared films in triplicate, as the replicated experimental units, and the mean and standard deviation of the property values were presented.

## 3. Results and discussion

### 3.1. Apparent film property

Flexible free-standing agar and agar/clay nanocomposite films were prepared by the solvent casting method. Transparency of the agar-based films determined by transmittance at 660 nm was affected greatly by formation of nanocomposite as shown in Fig. 1. The transmittance decreased significantly after incorporation of the nanoclay and the degree of decrease in the transmittance was dependent on the amount of the clay incorporated. The transmittance of the agar film decreased from 70.3% to 65.0% when 2.5% of the clay was added then decreased slowly with increase in clay content up to 15% of clay concentration followed by decreasing down to 51.9% with 20% of clay incorporation. In general, it is known that the transparency of a well-developed nanocomposite film is not significantly changed when the clay platelets with about one nm thick are well dispersed through the polymer matrix, since such clay platelets are less than the wavelength of visible light and do not hinder light's passage (Ogata et al., 1997). However, the large decrease in the transmittance of the agar nanocomposite films suggests that the nanoclay was not completely dispersed probably forming partial agglomeration in the polymer matrix especially at high concentration of clay incorporation and hindered light passage through the film.



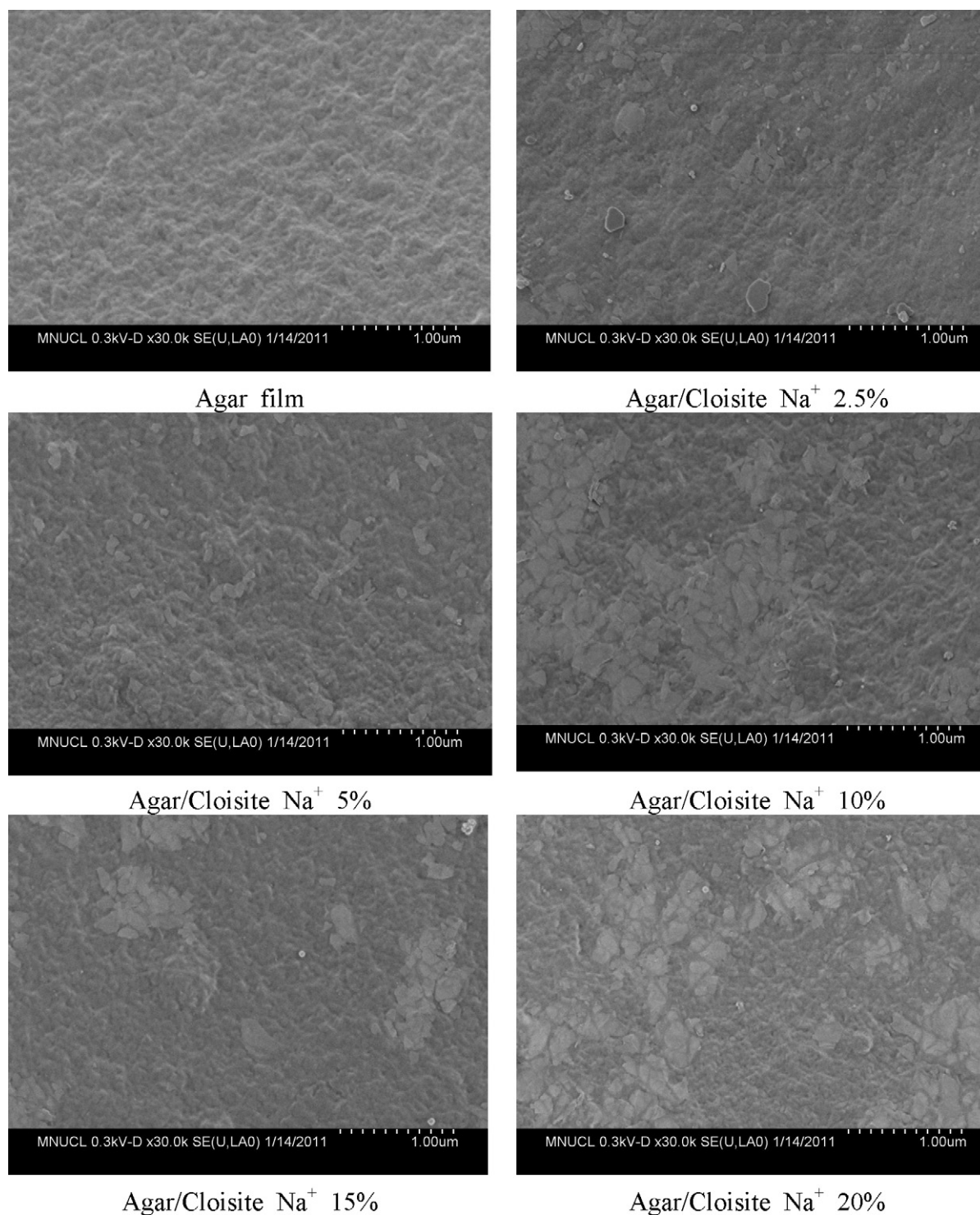


**Fig. 2.** Scanning electron micrographs of agar and agar/Cloisite Na<sup>+</sup> nanocomposite films prepared with different content of nanoclay.

### 3.2. Scanning electron microscopy

Microstructure of agar films was tested with scanning electron microscopy as shown in Fig. 2. SEM images indicate that high degree of dispersion of clay in the polymeric matrix was obtained at low level of clay content less than 5 wt% and noticeable clay agglomerates were observed with higher level of clay content above 10 wt%. This explains the previous result of distinctive decrease in transmittance of the nanocomposite films with high level of clay content (more than 10 wt%).

### 3.3. X-ray diffraction

The extent of dispersion and the intercalation of the nanoclay layers for the nanocomposite films were tested by XRD, which indicates a direct evidence of polymer chain confinement into the clay gallery. X-ray diffraction measurement results of the nanoclay (Cloisite Na<sup>+</sup>) and its agar nanocomposite films with different clay concentration are shown in Fig. 3. The XRD pattern of Cloisite Na<sup>+</sup> revealed the diffraction peak at  $2\theta$  was  $7.15^\circ$ , and it was shifted to lower angle around  $4.65\text{--}4.87^\circ$  after formation of nanocomposite

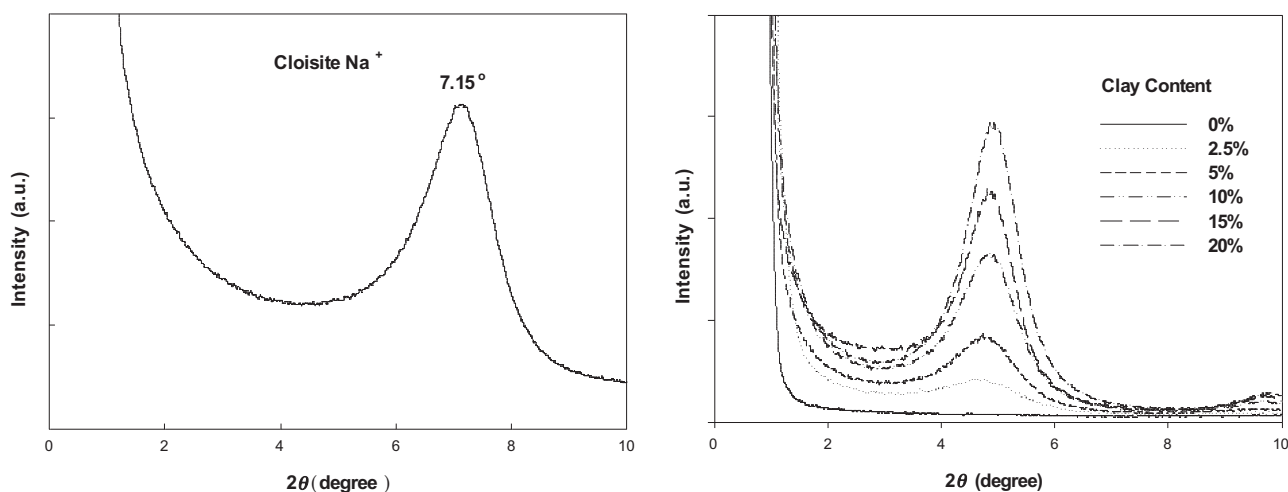


Fig. 3. X-ray diffraction patterns of clay (Cloisite Na<sup>+</sup>) and agar/Cloisite Na<sup>+</sup> nanocomposite films.

with agar polymer matrix. [Cyras et al. \(2008\)](#) also reported that the diffraction peak of Cloisite Na<sup>+</sup> was shifted to lower angles regardless of the clay content of starch/clay nanocomposite films. The angle of diffraction peak was not noticeably influenced by the clay concentration, but only intensity of the diffraction peak increased with increase in the clay concentration. Since the major portion of the nanocomposite films consists of the biopolymer matrix, the similar pattern of XRD was observed in all the nanocomposite films with different clay concentration, whereas only the intensity of the diffraction peaks varied. Similar trend of increase in peak intensity with increase in clay content was observed with ultrasonically treated solvent cast starch/CMC/Cloisite Na<sup>+</sup> nanocomposite films ([Alamsi et al., 2010](#)), and melt-intercalated starch-montmorillonite and starch-hectorite nanocomposite films ([Chen and Evans, 2005](#)).

The interlayer spacing (*d*-spacing) of the pristine nanoclay and those of nanocomposite films were determined using the Bragg's diffraction equation and the results are shown in [Table 1](#). The interlayer spacing of the nanoclay powder was 1.24 nm, which is close to the claimed value of the manufacturer (1.17 nm) and is in good agreement with the result (1.21 nm) of [Cyras et al. \(2008\)](#). The *d*-spacing of the clay increased from 1.24 nm to 1.81–1.90 nm after formation of agar/clay nanocomposite. This result indicates that the agar polymer chains entered into the silicate layers forming intercalated agar/clay nanocomposite without reaching complete exfoliation. This is probably due to the strong polar interaction between the agar polymer matrix and the silicate layers ([Cyras et al., 2008](#); [Park et al., 2002](#)). [Alamsi et al. \(2010\)](#) reported that the *d*-spacing of the silicate layers were 1.18 and 1.46 nm for the pristine and ultrasonically treated MMT, respectively, and it increased to 1.69 nm after formation of starch-CMC-clay nanocomposite with different amount of clay concentration from 1 to 7%. The degree of intercalation of their result is considerably lower than the present result, 1.69 nm vs. 1.81–1.90 nm. This indicates our nanocomposite preparation method of a series of hydration, high shear mixing, and

ultrasonication of clay solution is more favorable to develop higher degree of intercalation than the single ultrasonication method of [Alamsi et al. \(2010\)](#).

### 3.4. Surface roughness

Three dimensional AFM images are used to study detailed structure of the surface of film samples. Deflection of the cantilever in AFM observation measurement over *x* and *y* coordinate of the surface can be used to determine the average (*R<sub>a</sub>*) and root mean square roughness (*R<sub>q</sub>*) ([Rhim et al., 2011](#)). As shown in [Fig. 4](#), surface roughness of agar films was changed depending on the clay content. Surface roughness of agar films increased with increase in clay content up to 10% of clay incorporation then leveled off, which is probably attributed to the agglomeration of clay and embedded in the polymer matrix above the certain level of clay addition, i.e., 10%. Evidently the increase in surface roughness of the nanocomposite films with high content of clay indicates that the clay was not homogeneously mixed with agar polymer matrix as indicated in the SEM results.

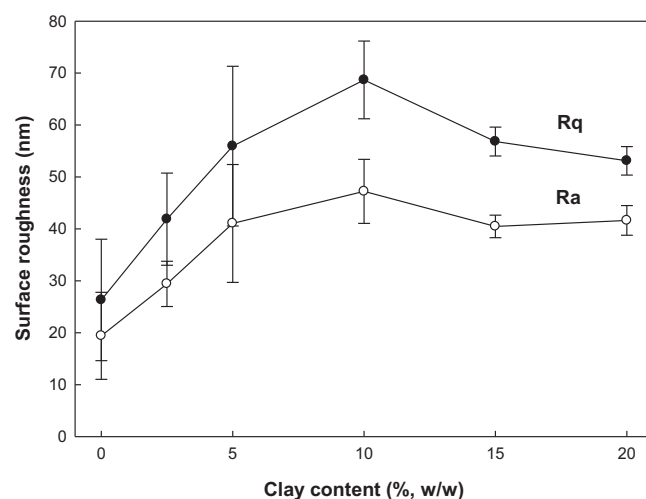


Fig. 4. Effect of clay content on surface roughness of agar/Cloisite Na<sup>+</sup> nanocomposite films.

**Table 1**  
Effect of clay content on gallery height of agar/Cloisite Na<sup>+</sup> nanocomposite films.

Clay content (% w/w)	2θ (deg.)	<i>d</i> -spacing (nm)
Cloisite Na <sup>+</sup>	7.15	1.24
0	No peak	–
2.5	4.65	1.90
5	4.87	1.81
10	4.83	1.83
15	4.81	1.84
20	4.85	1.82

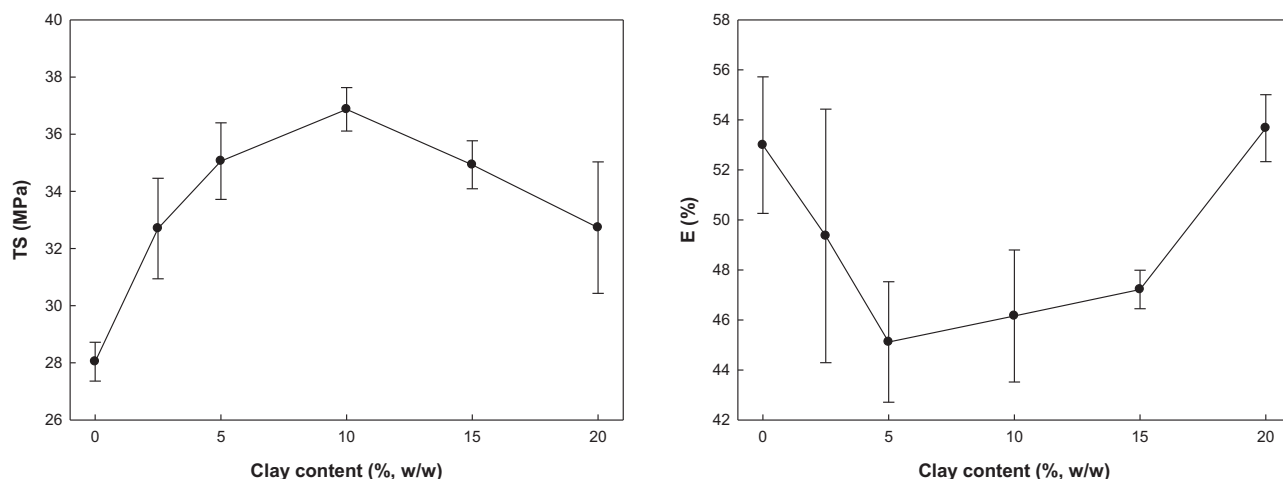


Fig. 5. Effect of clay content on tensile properties of agar/Cloisite Na<sup>+</sup> nanocomposite films.

### 3.5. Mechanical properties

Mechanical properties of agar and agar/clay nanocomposite films with various clay content resulted from the tensile test are shown in Fig. 5. The mechanical properties were also greatly influenced with the amount of clay addition. The TS of agar film increased from  $28.04 \pm 0.68$  MPa of the pure agar film (0% clay) up to  $36.87 \pm 0.76$  MPa with 10% addition then decreased with more addition of clay. A similar behavior of increase in TS with increase in the clay content have been observed in various biopolymer-based nanocomposite films such as starch (Alamsi et al., 2010; Avella et al., 2005; Cyras et al., 2008; De Carvalho et al., 2001; Huang et al., 2006), chitosan (Casariego et al., 2009), and soy protein (Kumar et al., 2010a,b). This behavior may be attributed to the resistance exerted not only by the clay itself with high surface area (about  $750 \text{ m}^2/\text{g}$ ), high aspect ratio (50–1000), and very high elastic modulus (178 GPa) (Alexandre and Dubois, 2000; Pandey et al., 2005; Pavlidou and Papaspyrides, 2008; Sinha Ray and Bousmina, 2005), but also by the stronger interfacial interaction through hydrogen or ionic bonds between polymer matrix and intercalated layered silicate with vast interfacial area (Alamsi et al., 2010). However, such reinforcing effect of clay was reduced above certain level of clay addition (10%), probably due to the formation of stacked clays without complete dispersion through polymer matrix at such high level of clay concentration. TS values of agar and agar/clay nanocomposite films are comparable to those commodity plastic films such as high density polyethylene (HDPE), polypropylene (PP), and polystyrene (PS), of which the TS values are in the range of 22–31, 31–38, and 45–83 MPa, respectively (Hernandez, Selke, & Culter, 2000).

On the contrary, ductility of the agar film, as determined in the E, exhibited reversed pattern of the TS. The E decreased with increase in clay content up to 5%, and increased above 5% of clay incorporation. However, the change in the E was not so distinctive; they were changed in a small range of 45.1–53.7%.

### 3.6. Water vapor permeability (WVP)

The water vapor barrier property of agar-based films determined by the WVP was also greatly influenced by the clay content used (Fig. 6A). The WVP of neat agar film was  $2.22 \pm 0.19 \text{ g m/m}^2 \text{ s Pa}$ . It decreased significantly with increase in the clay concentration down to  $1.07 \pm 0.05 \text{ g m/m}^2 \text{ s Pa}$  with the 20% of clay incorporation. Such phenomena of decrease in WVP with incorporation of nanoclays have frequently observed with various

biopolymers such as starch (Park, Lee, Park, Cho, & Ha, 2003), chitosan (Casariego et al., 2009; Rhim et al., 2006), soy protein (Kumar et al., 2010a,b), and whey protein (Sothornvit et al., 2010). It is generally known that the WVP of polymer/clay nanocomposite films decreases exponentially with increase in clay content or increase in aspect ratio of the clay (Yano, Usuki, & Okai, 1997). The decrease in WVP of polymer/clay composite films is mainly attributed to the tortuous path for water vapor diffusion due to the impermeable clay layers distributed in the polymer matrix with increasing the effective diffusion path length (Cussler, Hughes, Ward, & Aris, 1998; Sun, Boo, Clearfield, Sue, & Pham, 2008; Yano et al., 1997).

### 3.7. Contact angle (CA) of water

As one of the basic wetting properties, the CA of water droplet is measures the degree of hydrophilicity or hydrophobicity of surface of film, which is generally used to estimate the resistances of the film against liquid water (Phan et al., 2009; Rhim et al., 2006). Results on CA determination for the agar and agar/clay nanocomposite films are shown in Fig. 6B. The CA of neat agar film was  $47.05 \pm 0.05^\circ$ , and it decreased with increase in clay concentration in agar/Cloisite Na<sup>+</sup> nanocomposite films. Usually, the more hydrophilic a material is, the lower the CA value it has (Rhim et al., 2006). The decrease in the CA with increase in the clay concentration of agar/clay nanocomposite films was mainly due to the hydrophilic nature of the natural montmorillonite clay (Cloisite Na<sup>+</sup>). The CA of agar films is comparable to that of chitosan films ( $45.6 \pm 0.2^\circ$ ) (Rhim et al., 2006).

### 3.8. Water vapor absorption

Water vapor sensitivity of a film sample is evaluated by measuring water vapor absorption characteristics of the film. A water vapor absorption property of agar and agar/clay nanocomposite films was tested by measuring the water vapor uptake ratio (WVUR) under high water activity condition for 5 days using K<sub>2</sub>SO<sub>4</sub> saturated salt solution. Fig. 7A shows the results of the WVUR<sub>5</sub> of the agar and agar/clay nanocomposite films as a function of the clay content. The WVUR<sub>5</sub> of agar films decreased from  $227.3 \pm 12.5\%$  for the neat agar film as clay content increased. This result indicates that water vapor sensitivity property of the agar film is improved through nanocomposite formation with the nanoclay. Similar trend has been observed by the other researchers worked with starch/CMC/clay nanocomposite films (Alamsi et al., 2010) and starch/MMT nanocomposite films (Cyras et al., 2008). Cyras

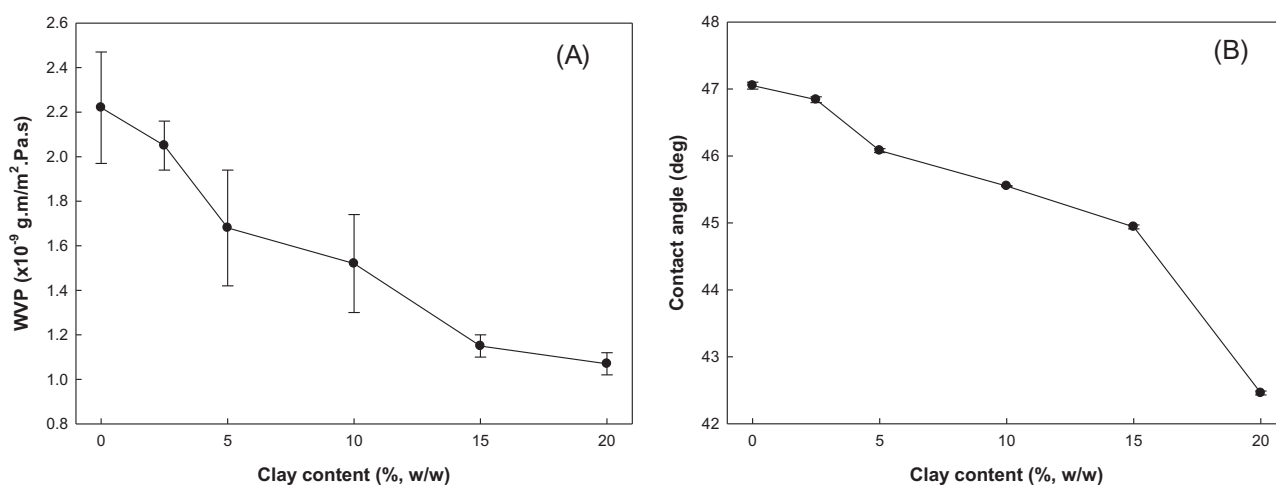


Fig. 6. Effect of clay content on (A) water vapor permeability (WVP) and (B) water contact angle (CA) of agar/Cloisite Na<sup>+</sup> nanocomposite films.

et al. (2008) tested water vapor uptake rate of starch films and their nanocomposite films with varying amount of MMT (2–5%) and determined the water vapor diffusion coefficient ( $D_{\text{eff}}$ ) to find that the water vapor absorption rate was slower for the nanocomposite films compared with the neat starch films. It is worthwhile to note

that the trend of decreasing the WVUR of the agar film with increasing the clay content is coincided with that of the WVP. Presumably, the decrease in WVUR of the nanocomposite films is partly due to the tortuous structure formed by the nanoclay dispersed through the polymer matrix.

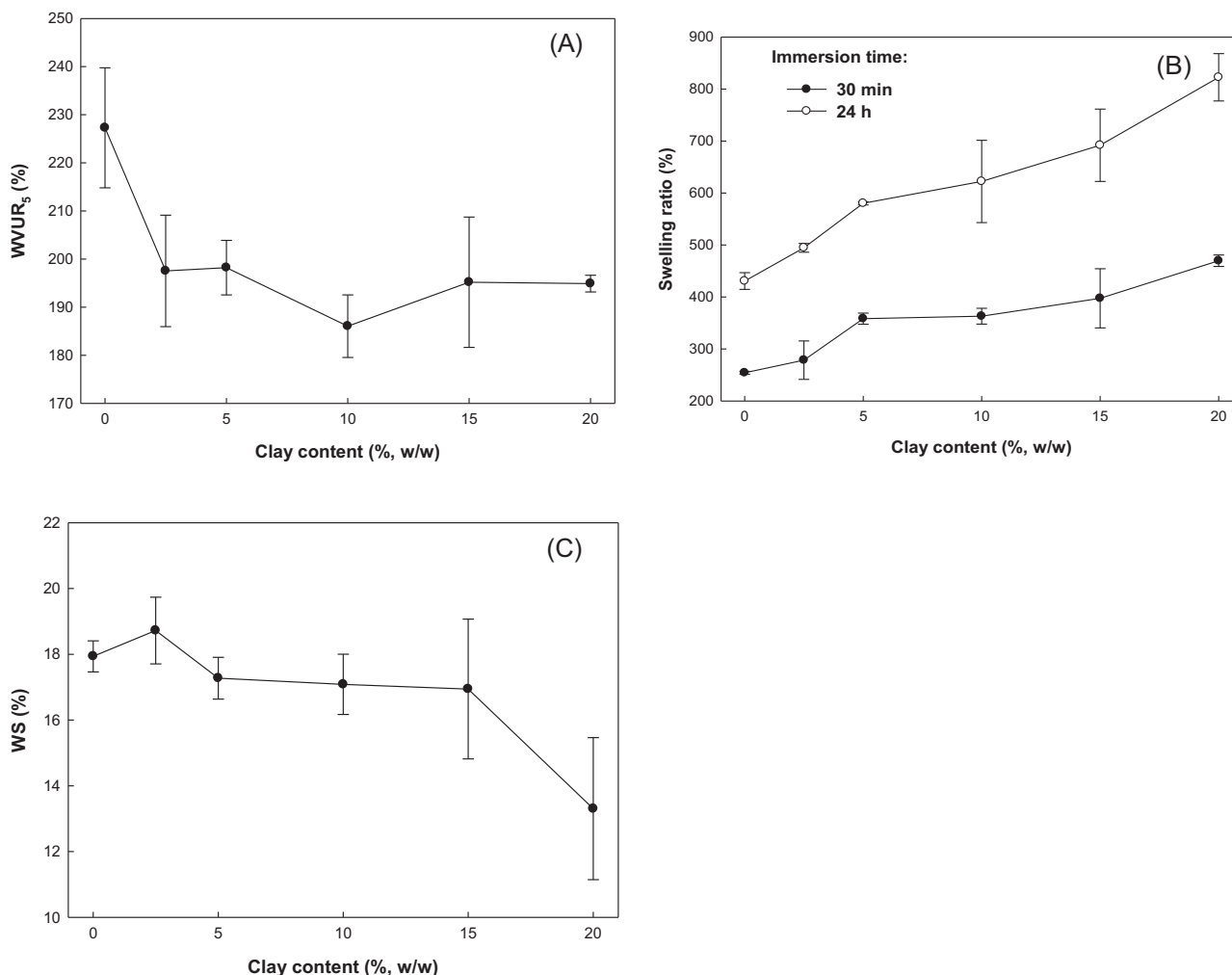


Fig. 7. Effect of clay content on (A) water vapor uptake ratio (WVUR), (B) swelling ratio (SR), and (C) water solubility (WS) of agar/Cloisite Na<sup>+</sup> nanocomposite films.



### 3.9. Water solubility (WS)

The WS is a measure of water soluble matter of a film sample, which is used as an indicator for the resistance of the film sample to water. Results on the WS of agar and agar/clay nanocomposite films as a function of clay content are shown in Fig. 7B. The WS of neat agar film was  $17.9 \pm 0.5\%$ . It decreased slightly with increase in the clay content down to  $16.9 \pm 2.1\%$  when the clay content was 15%, then it decreased substantially to  $13.8 \pm 2.16\%$  when the clay content was 20%. Such phenomena of decrease in WS with increase in clay content have been observed with different bionanocomposite such as starch/CMC/Cloisite Na<sup>+</sup> nanocomposite films (Alamsi et al., 2010) and chitosan/caly nanocomposite films (Casariego et al., 2009). This result indicates that water resistance of biopolymer films increased with incorporation of nanoclays. This is mainly due to the formation of strong interaction through hydrogen bonds between hydroxyl groups of the biopolymer matrix and nanoclays with high surface area, thus improving the cohesiveness of biopolymer matrix and decreasing the water sensitivity (Casariego et al., 2009).

### 3.10. Swelling ratio (SR)

The SR measures water holding capacity of a film sample. The SR measurements of the agar and agar/clay nanocomposite films after immersion in water for 30 min and 24 h as a function of clay contents are shown in Fig. 7C. The SR of agar films depends on both the immersion time and clay contents, i.e., the SR increased by more than 1.7 times with increase in the immersion time from 30 min to 24 h, and it also increased by about 1.8 times with increase in the clay content from 0 to 20% in both immersion times. The increase in SR with increase in the clay contents is probably due to the hydrophilic nature of the natural MMT clay. The high water holding capacity of the agar/Cloisite Na<sup>+</sup> nanocomposite film with increased mechanical strength and moderate flexibility can be used as a hydrogel (Farris, Schaich, Liu, Piergiovanni, & Yam, 2009).

## 4. Conclusions

Well developed bionanocomposite films were prepared with agar and different amounts of natural montmorillonite clay (Cloisite Na<sup>+</sup>) using a solvent intercalation method. Film properties of the nanocomposite films were greatly influenced by the clay content. XRD and SEM results revealed a higher degree of intercalation and dispersion of the clay in the polymer matrix with lower clay content (less than 5 wt%), while a clustering of agglomerates of clays at higher clay concentration above 10%. However, the mechanical strength (TS) of the agar film was the highest at 10% clay incorporated. Generally, the water vapor permeability (WVP), the water vapor uptake ratio (WVUR<sub>5</sub>), and the water solubility (WS) decreased with increase in the clay content due to formation of tortuous path for water vapor and development of strong interaction between the intercalated clay layers and the polymer matrix. The agar film became more hydrophilic with incorporation of the hydrophilic nanoclay, resulted in decrease in the water contact angle (CA) and increase in the swelling ratio (SW) with increase in clay content. These results indicate that film properties can be fine tuned for a specific application by choosing proper concentration of nanoclay. The agar/clay nanocomposite films with improved water vapor barrier and mechanical properties as well as controlled water resistance properties could be potentially used as environmentally friendly food packaging materials for extending the shelf-life, or as hydrogels using high water holding capacity with enhanced gel strength of the nanocomposite film.

## Acknowledgement

This research was supported by the Agriculture Research Center program of the Ministry for Food, Agriculture, Forestry and Fisheries, Korea.

## References

- Alexandre, M., & Dubois, P. (2000). Polymer-layered silicate nanocomposites: preparation, properties and use of new class of materials. *Materials Science and Engineering*, 28, 1–63.
- Alamsi, H., Ghanbarzadeh, B., & Entezami, A. A. (2010). Physicochemical properties of starch-CMC-nanoclay biodegradable films. *International Journal of Biological Macromolecules*, 46, 1–5.
- Avella, M., De Vlieger, J. J., Errico, M. E., Fischer, S., Vacca, P., & Volpe, M. G. (2005). Biodegradable starch/clay nanocomposite films for food packaging applications. *Food Chemistry*, 93, 467–474.
- Arora, A., & Padua, G. W. (2009). Review: Nanocomposites in food packaging. *Journal of Food Science*, 75(1), R43–R49.
- Bae, H. J., Park, H. J., Hong, S. I., Byun, Y. J., Darby, D. O., Kimmel, R. M., et al. (2009). Effect of clay content, homogenization RPM, pH, and ultrasonication on mechanical and barrier properties of fish gelatin/montmorillonite nanocomposite films. *LWT-Food Science and Technology*, 42, 1179–1186.
- Boredes, P., Pollet, E., & Avérous, L. (2009). Nano-biocomposites: biodegradable polyester/nanoclay systems. *Progress in Polymer Science*, 34, 125–155.
- Brody, A. (2003). Nanocomposite technology in food packaging. *Food Technology*, 61(10), 80–83.
- Cabedo, L., Feijoo, J. L., Villanueva, M. P., Lagarón, J. M., & Giménez, E. (2006). Optimization of biodegradable nanocomposites based on PLA/PCL blends for food packaging applications. *Macromolecular Symposia*, 233, 191–197.
- Casariego, A., Souza, B. W. S., Cerqueira, M. A., Teixeira, J. A., Cruz, L., Díaz, R., et al. (2009). Chitosan/clay film's properties as affected by biopolymer and clay micro/nanoparticles' concentrations. *Food Hydrocolloids*, 23, 1895–1902.
- Chen, B., & Evans, J. R. G. (2005). Thermoplastic starch-clay nanocomposites and their characteristics. *Carbohydrate Polymers*, 61, 455–463.
- Cussler, E. L., Highes, S. E., Ward, W. J., & Aris, R. (1998). Barrier membranes. *Journal of Membrane Science*, 38, 161–174.
- Cyras, V. P., Manfredi, L. B., Ton-That, M. T., & Vázquez, A. (2008). Physical and mechanical properties of thermoplastic starch/montmorillonite nanocomposite films. *Carbohydrate Polymer*, 73, 55–63.
- De Carvalho, A. J. F., Curvelo, A. A. S., & Agnelli, J. A. M. (2001). A first insight on composites of thermoplastic starch and kaolin. *Carbohydrate Polymers*, 45, 189–194.
- De Mesquita, J. P., Donnici, C. L., & Pereira, F. V. (2010). Biobased nanocomposites from layer-by-layer assembly of cellulose nanowhiskers with chitosan. *Biomacromolecules*, 11, 473–480.
- Farris, S., Schaich, K. M., Liu, L., Piergiovanni, L., & Yam, K. L. (2009). Development of polyion-complex hydrogels as an alternative approach for the production of bio-based polymers for food packaging applications: A review. *Trends in Food Science & Technology*, 20, 316–332.
- Freile-Pelegrín, Y., Mader-Santana, T., Robledo, D., Veleza, L., Quintana, P., & Azamar, J. A. (2007). Degradation of agar films in a humid tropical climate: Thermal, mechanical, morphological and structural changes. *Polymer Degradation and Stability*, 92, 244–252.
- Gennadios, A., Weller, C. L., & Gooding, C. H. (1994). Measurement errors in water vapor permeability of high permeable, hydrophilic edible films. *Journal of Food Engineering*, 21, 395–409.
- Gontard, N., Guilbert, S., & Cuq, J. L. (1992). Edible wheat gluten films: Influence of the main process variables on film properties using response surface methodology. *Journal of Food Science*, 57, 190–195, 199.
- Hedenqvist, M. S., Backman, A., Gällstedt, M., Boyd, R. H., & Gedde, U. W. (2006). Morphology and diffusion properties of whey/montmorillonite nanocomposites. *Composites Science and Technology*, 66, 2350–2359.
- Hernandez, R. J., Selke, S. E. M., & Culter, J. D. (2000). Major plastics in packaging. In *Plastics packaging*. Cincinnati: Hanser Gardner Publications, Inc., pp. 89–134.
- Huang, M., Yu, J., & Ma, X. (2006). High mechanical performance MMT-urea and formamide-plasticized thermoplastic cornstarch biodegradable nanocomposites. *Carbohydrate Polymers*, 63, 393–399.
- Jang, S. A., Lim, K. O., & Song, K. B. (2010). Use of nano-clay (Cloisite Na<sup>+</sup>) improves tensile strength and vapor permeability in agar rich red algae (*Gelidium corneum*)-gelatin composite films. *International Journal of Food Science & Technology*, 45, 1883–1888.
- Kumar, P., Sandeep, K. P., Alavi, S., Truong, V. D., & Gorga, R. E. (2010a). Preparation and characterization of bio-nanocomposite films based on soy protein isolate and montmorillonite using melt extrusion. *Journal of Food Engineering*, 100, 480–489.
- Kumar, P., Sandeep, K. P., Alavi, S., Truong, V. D., & Gorga, R. E. (2010b). Effect of type and content of modified montmorillonite on the structure and properties of bio-nanocomposite films based on soy protein isolate and montmorillonite. *Journal of Food Science*, 75, N46–N56.
- Labropoulos, K. C., Niesz, D. E., Danforth, S. C., & Kevrekidis, P. G. (2002). Dynamic rheology of agar gels: Theory and experiment. Part I. Development of a rheological model. *Carbohydrate Polymers*, 50, 393–406.
- Lee, J. P., Lee, K. H., & Song, H. K. (1997). Manufacture of biodegradable packaging foams from agar by freeze-drying. *Journal of Materials Science*, 32, 5825–5832.



- Letendre, M., D'Aprano, G., Lacroix, M., Salmieri, S., & Sr-Gelais, D. (2002). Physicochemical properties and bacterial resistance of biodegradable milk protein films containing agar and pectin. *Journal of Agricultural and Food Chemistry*, 50, 6017–6022.
- Mauricio-Iglesias, M., Peyron, S., Guillard, V., & Gontard, N. (2010). Wheat gluten nanocomposite films as food-contact materials: Migration tests and impact of a novel food stabilization technology (high pressure). *Journal of Applied Polymer Science*, 116, 2526–2535.
- Müller, C. M. O., Laurindo, J. B., & Yamashita, F. (2011). Effect of nanoclay incorporation method on mechanical and water vapor barrier properties of starch-based films. *Industrial Crops and Products*, 33, 605–610.
- Ogata, N., Jimenez, G., Kawai, H., & Ogihara, T. (1997). Structure and thermal/mechanical properties of poly(L-lactide)-clay blend. *Journal of Polymer Science Part B: Polymer Physics*, 35, 389–396.
- Pandey, J. K., Kumar, A. P., Misra, M., Mohanty, A. K., Drzal, L. T., & Singh, R. P. (2005). Recent advances in biodegradable nanocomposites. *Journal of Nanoscience and Nanotechnology*, 5, 497–526.
- Park, H. M., Li, X., Jin, C. Z., Park, C. Y., Cho, W. J., & Ha, C. S. (2002). Preparation and properties of biodegradable thermoplastic starch/clay hybrids. *Macromolecular Materials and Engineering*, 287, 553–558.
- Park, H. M., Lee, W. K., Park, C. Y., Cho, W. J., & Ha, C. S. (2003). Environmentally friendly polymer hybrids. Part I. Mechanical, thermal, and barrier properties of thermoplastic starch/clay nanocomposites. *Journal of Materials Science*, 38, 909–915.
- Park, H. M., Liang, X., Mohanty, A. K., Manjusri, M., & Drzal, L. T. (2004). Effect of compatibilizer on nanostructure of the biodegradable cellulose acetate/organoclay nanocomposites. *Macromolecules*, 37, 9076–9082.
- Pavlidou, S., & Papaspyrides, C. D. (2008). A review on polymer-layered silicate nanocomposites. *Progress in Polymer Science*, 33, 1119–1198.
- Petersson, L., & Oksman, K. (2006). Biopolymer based nanocomposites: comparing layered silicates and microcrystalline cellulose as nanoreinforcement. *Composites Science and Technology*, 66, 2187–2196.
- Phan, T. D., Debeaufort, F., Luu, D., & Voilley, A. (2005). Functional properties of edible agar-based and starch-based films for food quality preservation. *Journal of Agricultural and Food Chemistry*, 53, 973–981.
- Phan, T. D., Debeaufort, F., Voilley, A., & Luu, D. (2009). Biopolymer interactions affect the functional properties of edible films based on agar, cassava and arabinoxylan blends. *Journal of Food Engineering*, 90, 548–558.
- Rao, Y. Q. (2007). Gelatin–clay nanocomposites of improved properties. *Polymer*, 48, 5369–5375.
- Rhim, J. W., Hong, S. I., Park, H. M., & Ng, P. K. W. (2006). Preparation and characterization of chitosan-based nanocomposite films with antimicrobial activity. *Journal of Agricultural and Food Chemistry*, 54, 5814–5822.
- Rhim, J. W., & Ng, P. K. W. (2007). Natural biopolymer-based nanocomposite films for packaging applications. *Critical Reviews in Food Science and Nutrition*, 47, 411–433.
- Rhim, J. W., Lee, S. B., & Hong, S. I. (2011). Preparation and characterization of agar/clay nanocomposite films: The effect of clay type. *Journal of Food Science*, 76(3), N40–N48.
- Sinha Ray, S., & Bousmina, M. (2005). Biodegradable polymers and their layered silicate nanocomposites: In greening the 21st century materials world. *Progress in Materials Science*, 50, 962–1079.
- Siracusa, V., Rocculi, P., Romani, S., & Rossa, M. D. (2008). Biodegradable polymers for food packaging: A review. *Trends in Food Science & Technology*, 19, 634–643.
- Sorrentiono, A., Gorras, G., & Vittoria, V. (2007). Potential perspectives of biodegradable nanocomposites for food packaging applications. *Trends in Food Science & Technology*, 18, 84–95.
- Sothornvit, R., Hong, S. I., An, D. J., & Rhim, J. W. (2010). Effect of clay content and antimicrobial properties of whey protein isolate/organoclay composite films. *LWT-Food Science and Technology*, 43, 279–284.
- Sun, L., Boo, W. J., Clearfield, A., Sue, H. J., & Pham, H. Q. (2008). Barrier properties of model epoxy nanocomposites. *Journal of Membrane Science*, 318, 129–136.
- Tunc, S., Angellier, H., Cahyana, Y., Chalier, P., Gontard, N., & Gastaldi, E. (2007). Functional properties of wheat gluten/montmorillonite nanocomposite films processed by casting. *Journal of Membrane Science*, 289, 159–168.
- Weber, C. J., Haugaard, V., Festersen, R., & Bertelsen, G. (2002). Production and application of biobased packaging materials for the food industry. *Food Additives and Contaminations*, 19(Suppl.), 172–177.
- Wu, Y., Geng, F., Chang, P. R., Yu, J., & Ma, X. (2009). Effect of agar on microstructure and performance of potato starch film. *Carbohydrate Polymers*, 76, 299–304.
- Yano, K., Usuki, A., & Okai, A. (1997). Synthesis and properties of polyimide-clay hybrid films. *Journal of Polymer Science Part A: Polymer Chemistry*, 35, 2289–2294.
- Zhou, J. J., Wang, S. Y., & Gunasekaran, S. (2009). Preparation and characterization of whey protein film incorporated with TiO<sub>2</sub> nanoparticles. *Journal of Food Science*, 74(7), N50–N56.